Phycological Research

Phycological Research 2022 doi: 10.1111/pre.12502

Prorocentrum pervagatum sp. nov. (Prorocentrales, Dinophyceae): A new, small, planktonic species with a global distribution

Urban Tillmann [1]*, **Stephan Wietkamp** [1], **Marc Gottschling** [2] **and Mona Hoppenrath**[3]

[1]Alfred Wegener Institute for Polar and Marine Research, Bremerhaven, Germany, [2]Department Biology, Systematics, Biodiversity and Evolution of Plants, GeoBio-Center, Ludwig Maximilian University Munich, Munich, Germany and [3]Senckenberg am Meer, German Centre for Marine Biodiversity Research (DZMB), Wilhelmshaven, Germany

SUMMARY

Prorocentrum comprises a unique group of dinophytes with several apomorphic traits, such as an apical insertion of flagella and the presence of two major, large thecal plates. Species delimitation is challenging, especially for morphologically very similar, small planktonic species. Contemporary analyses, including SEM studies and molecular phylogenetics of type material, are not available for many described species. Based on six strains isolated from Antarctic, subarctic and North Atlantic waters, *Prorocentrum pervagatum* sp. nov. is described. *Prorocentrum pervagatum* was small (12–16 μm long and deep), oval to round in outline, and moderately compressed. One small, pyrenoid-like structure was faintly visible in some cells. Rod-like, long trichocysts were present. Cells had one distinct apical spine (1.1–1.7 μm in length) visible in light microscopy. The plate surface appeared smooth in light microscopy with few pores located close to the plate margin visible in empty thecae. Electron microscopy revealed plates to be densely covered by small projections and two size classes of thecal pores. Cells had a row of mostly four large pores in apical-ventral position on the right thecal plate. The periflagellar area consisted of eight small platelets. The apical spine was formed by platelet six. In molecular phylogenetics, *P. pervagatum* was part of a species group generally exhibiting small size and spiny thecal ornamentation, together with *Prorocentrum cordatum* and *Prorocentrum obtusidens*. The new species is distinct in DNA trees and differs from the protologues of other small species of *Prorocentrum* by the unique combination of size, shape (i.e. only moderately compressed or round), presence of a distinct apical spine, and position of thecal pores (i.e. located at the plate margins only). Its clear description and illustration may stimulate similar work of other small species of *Prorocentrum*, particularly including the re-investigation of taxa with historical names collected at the corresponding type localities.

Key words: biogeography, dinoflagellate, morphology, periflagellar area, phylogeny, plankton, protist, taxonomy.

INTRODUCTION

Prorocentrum comprises a diverse and primarily marine group of dinophytes with a worldwide distribution (Dodge 1975). In addition to the type species *Prorocentrum micans* Ehrenberg, there are about 80 taxonomically accepted species (Guiry & Guiry 2022). A number of planktonic members of *Prorocentrum*, such as *P. micans*, *Prorocentrum cordatum* (Ostenfeld) J.D.Dodge [= *Prorocentrum minimum* (Pavillard) J.Schiller], or *Prorocentrum obtusidens* J.Schiller [= *Prorocentrum donghaiense* D.Lu], are important bloom formers in coastal areas all over the world (Heil *et al*. 2005; Shin *et al*. 2019; Tillmann *et al*. 2019). Species of *Prorocentrum* are phototrophic or mixotrophic (Hansen & Tillmann 2020). It is said that there are no fossils of Prorocentrales (Fensome *et al*. 1993), but the group has been dated to the Lower Cretaceous (Chacón & Gottschling 2020). The Prorocentrales have a peculiar morphology characterized by the presence of two major large thecal plates with a distinct sagittal suture, the lack of cingulum and sulcus, and an apical insertion of flagella (desmokont flagellation) (Dodge 1975). Both flagella arise in the periflagellar area from one flagellar pore, which is surrounded by an apical cluster of 5–14 platelets and accompanied by an accessory pore (Hoppenrath *et al*. 2013). Morphological determination of species is historically based on size, shape, surface ornamentation of the thecal plates, number and distribution of thecal pores, and the presence/absence of conspicuous apical projections (Dodge 1975). It is now increasingly supplemented by ultrastructural details of the periflagellar area (Hoppenrath *et al*. 2013; Chomérat *et al*. 2019; Tillmann *et al*. 2019, 2022), which have not been accurately studied in many original descriptions.

In fact, most of the planktonic species have been described before 1980 and observed using light microscopy (LM) only. Thus, detailed information of the ultrastructure and DNA sequence data are lacking for the types, or physical material is entirely lacking. This is especially critical for small (<20 μm), circular, and inconspicuous species, for which the diagnostic traits are difficult to observe reliably by LM. Therefore, some crucial features have been overlooked or described ambiguously before. For example, thecal surface

*To whom correspondence should be addressed.
Email: urban.tillmann@awi.de
Received 4 June 2022; accepted 16 September 2022.

ornamentation such as tiny projections have been originally recognized as minute pores (Ostenfeld 1902; Pavillard 1916). Moreover, minute apical projections (which in any case are difficult to observe in LM) have been described with different terms such as spine, wing, tooth (Schiller 1933), or equivalent.

A perspicuous example for the challenges referring to unambiguous identification of small species of *Prorocentrum* is strain PLY 184 (= LB1008). It was initially deposited and published (Dodge & Bibby 1973) as *Prorocentrum pusillum* (J.Schiller) J.D.Dodge & B.T.Bibby, and the determination was changed in 1976 to *Prorocentrum nanum* J.Schiller (Starr & Zeikus 1993). This goes back to the synonymization of *P. nanum* and *P. pusillum* shortly before (Dodge 1975), although the two species are distinct in LM (Puigserver & Zingone 2002). Finally, strain PLY 184 turned out to represent a distinct species, namely *Prorocentrum nux* Puigserver & Zingone, which can be differentiated by careful LM from both *P. pusillum* and *P. nanum* (Puigserver & Zingone 2002).

Fourteen small (<20 μm) and in outline round or oval species of *Prorocentrum* are readily distinguished (occasionally introduced under *Exuviaella*), namely *Exuviaella aequatorialis* Hasle, *Prorocentrum antarcticum* (Hada) Balech, *Prorocentrum balticum* (Lohmann) A.R.Loeblich, *P. cordatum*, *Prorocentrum cordiforme* Bursa, *Prorocentrum cornutum* J. Schiller, *P. nanum*, *P. nux*, *Prorocentrum pomoideum* Bursa, *Prorocentrum ponticum* Krakhmalny & Terenko (*nom. corr.*: ICN Art. 23.5), *P. pusillum*, *Prorocentrum ovum* (J.Schiller) J.D.Dodge, *Prorocentrum rotundatum* J.Schiller, and *Prorocentrum sphaeroideum* J.Schiller. However, type or original material of only *P. nux* has been studied using both LM and electron microscopy (EM) (Puigserver & Zingone 2002) but even here the only sequence data available in GenBank are from strain RCC303 (without published morphological documentation) and not from strain pronap1, from which the type was prepared. For another recently described small species of *Prorocentrum*, *P. ponticum*, low-resolution scanning electron microscopy (SEM) is provided only, but no LM images, no drawings, and no DNA sequence data are reported (Krakhmalny & Terenko 2004). Concluding, unambiguous names are currently not given for small, in outline roundish species of *Prorocentrum*, with severe implications for the assessment of diversity, biogeography, taxonomy, and synonymy.

The present study describes a new small species of *Prorocentrum* and determines the systematic placement in molecular phylogenetics of the Prorocentrales. The group is difficult to capture as inferred from DNA sequence data (Murray *et al*. 2009; Tillmann *et al*. 2012) because of strong rate heterogeneity, but is monophyletic in analyses using concatenated sequences of the ribosomal RNA (rRNA) operon (Hoppenrath *et al*. 2013; Chacón & Gottschling 2020; Gottschling *et al*. 2020). The morphology of the new species allows sufficient differentiation from other, similar-sized species of *Prorocentrum*. The description is based on strains isolated from different areas, ranging from Antarctic and subarctic waters to the North Sea, indicating a rather wide geographical distribution and broad ecological amplitude of this new species.

MATERIALS AND METHODS

Sampling, cell isolation, cultivation

Six strains of *Prorocentrum pervagatum* sp. nov. (Table 1) from four different areas (Fig. 1) were established in the course of this study. Strain CA-01 was established from a sample taken in Potter Cove, King George Island, South Shetland Islands, Western Antarctic Peninsula (Fig. 1) during a stay at the Research laboratory 'Dallmann' of the Alfred-Wegener-Institute for Polar and Marine Research, which is associated with the Argentine research station Carlini. Strain PM-01 was obtained from the central Labrador Sea onboard *RV Maria S. Merian* (research cruise MSM65). For a plankton field sample analysis of the Labrador Sea station, Niskin bottle samples of three depths (3 m, 10 m, and depth of the chlorophyll maximum) were taken and pooled. Subsamples were fixed with Lugol's iodine (1% final concentration) for quantitative plankton analysis, and 50 and 10 mL were settled in Utermöhl sedimentation chambers and counted with an IMR inverted microscope (Olympus; Hamburg, Germany). Another 1-L sub-sample was gently concentrated by gravity filtration using a 5-μm polycarbonate filter (47 mm diameter, Millipore, Eschborn, Germany), and the concentrate was fixed with formaldehyde (1% final concentration) for later SEM analysis. Two additional strains (P3-B7 and P3-C7) were obtained from the Norwegian coast during a research survey with *RV Heincke* (HE448) (Table 1). Strains LP-D3 and LP-D10 were isolated during a cruise with *RV Uthörn* (UTH2020) from water collected in coastal waters of the southern North Sea off Denmark (Fig. 1, Table 1).

All strains of *Prorocentrum* were obtained by single-cell isolation using micropipettes under a stereomicroscope (M5A, Wild, Heerbrugg, Switzerland). Cells were transferred into individual wells of 96-well tissue culture plates (TPP, Trasadingen, Switzerland) each containing 250 μL of K-medium (Keller *et al*. 1987) prepared from 0.2-μm sterile-filtered natural Antarctic seawater diluted 1:10 with filtered seawater from the sampling location. The original K-medium recipe was slightly modified by replacing the organic phosphorus source with 3.62 μM Na_2HPO_4. Plates were incubated at 10°C under dim light (30 μmol photons m^{-2} s^{-1}) in a controlled environment growth chamber (MIR 252, Sanyo Biomedical; by Wood Dale, USA). After 3–4 weeks, all strains were inoculated for batch cultures in 65-mL polystyrene cell culture flasks. Growth medium was enriched with nutrients corresponding to 50% of the modified K-medium.

For DNA harvest, cells were collected by centrifugation (5810R, Eppendorf; Hamburg, Germany) in 50-mL centrifugation tubes at 3220 g for 10 min. Cell pellets were transferred into 1-mL microtubes, again centrifuged (5415, Eppendorf; 16 000 g, 5 min), and stored at −20°C for subsequent DNA extraction.

Microscopy

Observation of living or fixed cells (formaldehyde- or neutral Lugol-fixed, 1% final concentration) was carried out using an inverted microscope (Axiovert 200M, Zeiss; Jena, Germany) and a compound microscope (Axiovert 2, Zeiss), both equipped with epifluorescence and differential interference contrast optics. Thecal plates were examined using

Table 1. *Prorocentrum pervagatum* sp. nov.: compilation of strain information

Strain	Isolation date	Origin	Coordinates	Survey, sample, depth, temperature, salinity
CA-01	January 2014	Western Antarctic Peninsula	62°14.24′ S; 58°42.05′ W	Dallmann stay, 2014, bottle sample, surface, 2.0°C, 34.1
P3-B7	July 2015	Norwegian coast	59°18.56′ N; 04°57.93′ E	He448, 2015, Stat 9, bottle sample, 3 m, 12.5°C, 31.9
P3-C7	July 2015	Norwegian coast	59°18.56′ N; 04°57.93′ E	He448, 2015, Stat 9, bottle sample, 3 m, 12.5°C, 31.9
PM-01	June 2017	Labrador Sea	56°49.42′ N; 52°13.15′ W	MSM65, 2017, Stat 01, bottle sample, 10 m, 7.0°C, 34.6
LP-D3	June 2020	German Bight	56°37.41′ N; 06°41.27′ E	UTH2020, Stat 5, bottle sample, 3 m, 17.8°C, 34.5
LP-D10	June 2020	German Bight	56°37.41′ N; 06°41.27′ E	UTH2020, Stat 5, bottle sample, 3 m, 17.8°C, 34.5

epifluorescence microscopy of cells stained either with calcofluor white (Fritz & Triemer 1985) or with Solophenyl Flavine 7GFE500 (Chomérat *et al.* 2017). The shape and location of the nucleus were determined after staining of formalin-fixed cells with 4′-6-diamidino-2-phenylindole (DAPI, 0.1 μg mL^{-1} final concentration) for 10 min. Images were taken with a digital camera (Axiocam MRc5, Zeiss).

The length and depth of freshly fixed cells (neutral Lugol) from dense but healthy and growing strains (based on stereomicroscopic inspection of living material) during the late exponential phase were measured at a microscopic magnification of 640× using the inverted microscope and Axiovision software (Zeiss).

For SEM, cells of all strains were collected by centrifugation (5810R, Eppendorf; 3220 g for 10 min) from 15 mL of the strain. The supernatant was removed, and the cell pellet was re-suspended in 60% ethanol prepared in a 2-mL microtube with seawater (final salinity ca. 13) at 4°C for 1 h in order to strip off the outer cell membrane. Cells were further collected by centrifugation (5415R, Eppendorf; 16 000 g for 5 min), re-suspended and fixed in a 60:40 mixture of deionized water and seawater (final salinity ca. 13) with the addition of formaldehyde (1% final concentration), and stored at 4°C for 3 h. In addition, the formaldehyde-fixed field sample (plankton concentrate) obtained from Station 1 of the central Labrador Sea was examined by SEM as well. Cells from all samples were collected on polycarbonate filters (25 mm Ø, 3 μm pore size, Millipore Merck; Darmstadt, Germany) in a filter funnel, in which all subsequent washing and dehydration steps were carried out. A total of eight washing steps (2 mL MilliQ-deionized water each) were followed by a dehydration series in ethanol (30, 50, 70, 80, 95, and 100%; 10 min each). Filters were dehydrated with hexamethyldisilazane (HMDS), first in 1:1 HMDS:EtOH and then twice in 100% HMDS, and then stored in a desiccator under gentle vacuum. Finally, filters were mounted on stubs, sputter-coated (Emscope SC500, Ashford, UK) with gold–palladium, and viewed by SEM at 10 kV (FEI Quanta FEG 200, Eindhoven, the Netherlands). Micrographs were presented on a black background using Photoshop 6.0 (Adobe Systems, San Jose, CA, USA).

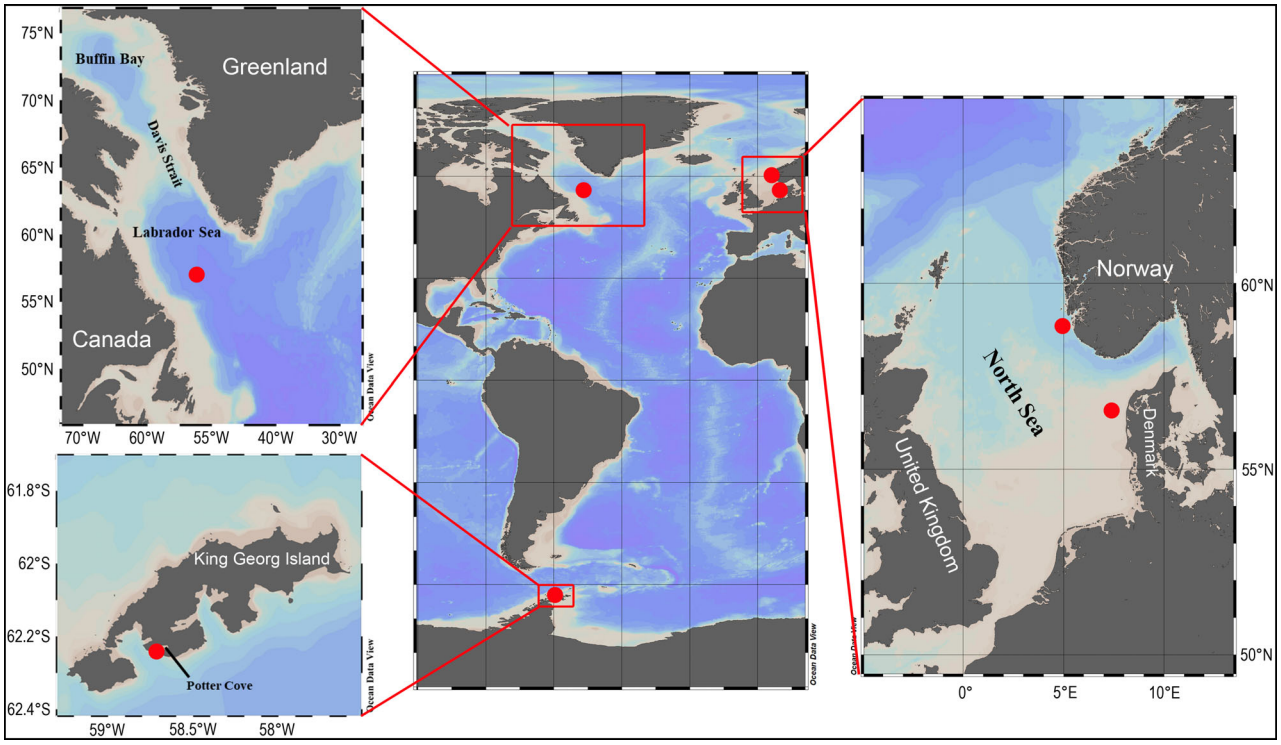

Fig. 1. Study area and sampling locations for different strains of *Prorocentrum pervagatum* sp. nov. obtained from the central Labrador Sea in June 2017 (upper left), from Potter Cove, King George Island, in January 2014 (lower left), and from the North Sea area off Norway in July 2015 and off Denmark in June 2020 (both on the right).

SEM pictures were used to determine for all strains the mean areal density of knob-like, conical projections on the lateral plates. Knobs were manually counted on randomly placed sections of 3 × 3 μm on images of plain plates from at least 20 different cells.

DNA sequencing

Genomic DNA was extracted from harvested fresh material using the Nucleo Spin Plant II Kit (Macherey-Nagel; Düren, Germany) according to the manufacturers' instructions. The DNA extract was stored at −20°C until further processing.

Sanger sequencing of DNA was performed for various regions of the rRNA operon, including the 18S/small subunit rRNA gene (SSU), the Internal Transcribed Spacer region (ITS1, 5.8S rRNA gene, ITS2), and the D1/D2 region of the 28S/large subunit rRNA gene (LSU), using published primer sets for SSU (Medlin *et al*. 1988), ITSa and ITSb (Adachi *et al*. 1996), and LSU (Scholin *et al*. 1994).

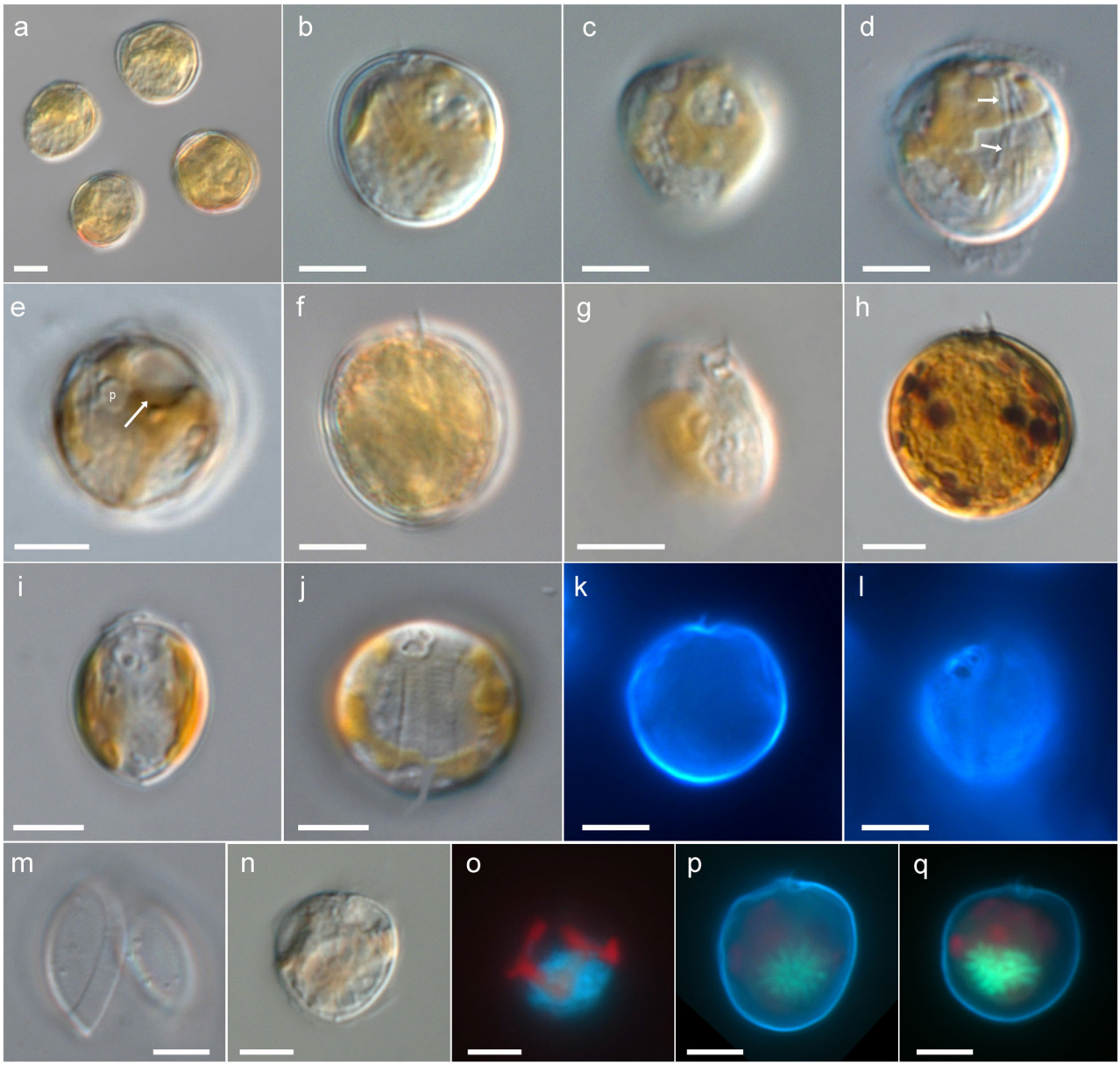

Fig. 2. *Prorocentrum pervagatum* sp. nov., strain PM-01. LM of living cells (a–g, i, j), a Lugol-fixed cell (h), or formaldehyde-fixed cells (k–q). (a–j) Different cells in lateral view (b–f, h), in lateral apical view (g), or in dorsal/ventral view (i, j). Note the pusule [white arrow in (e)], long trichocyst rods [white arrow in (d)], a presumable pyrenoid (p) in (e), and the broad growth band in (j). (k, l) Cells stained with calcofluor white and viewed with epifluorescence and UV light excitation in lateral view (k) or apical view (l). (m) Empty theca. Note the visibility of thecal pores close to the plate margins. (n, o) The same cell DAPI-stained and viewed with regular light (n) or with epifluorescence and UV excitation (o) to indicate the shape and location of the nucleus (blue). (p, q) Different cells simultaneously stained with calcofluor white and DAPI to indicate the posterior position of the nucleus. Scale bars: 5 μm.

PCR analysis was conducted in a Nexus Gradient Mastercycler (Eppendorf) as described in Tillmann *et al*. (2020), and PCR amplicons were inspected on a 1% agarose gel (in TE buffer, 70 mV, 30 min) to verify the expected length. Amplicons were purified following the instructions of the NucleoSpin Gel and PCR clean-up kit (Macherey-Nagel) and were sequenced directly in both directions on an ABI PRISM 3730XL (Applied Biosystems by Thermo Fisher Scientific; Waltham, USA) as described in Tillmann *et al*. (2017).

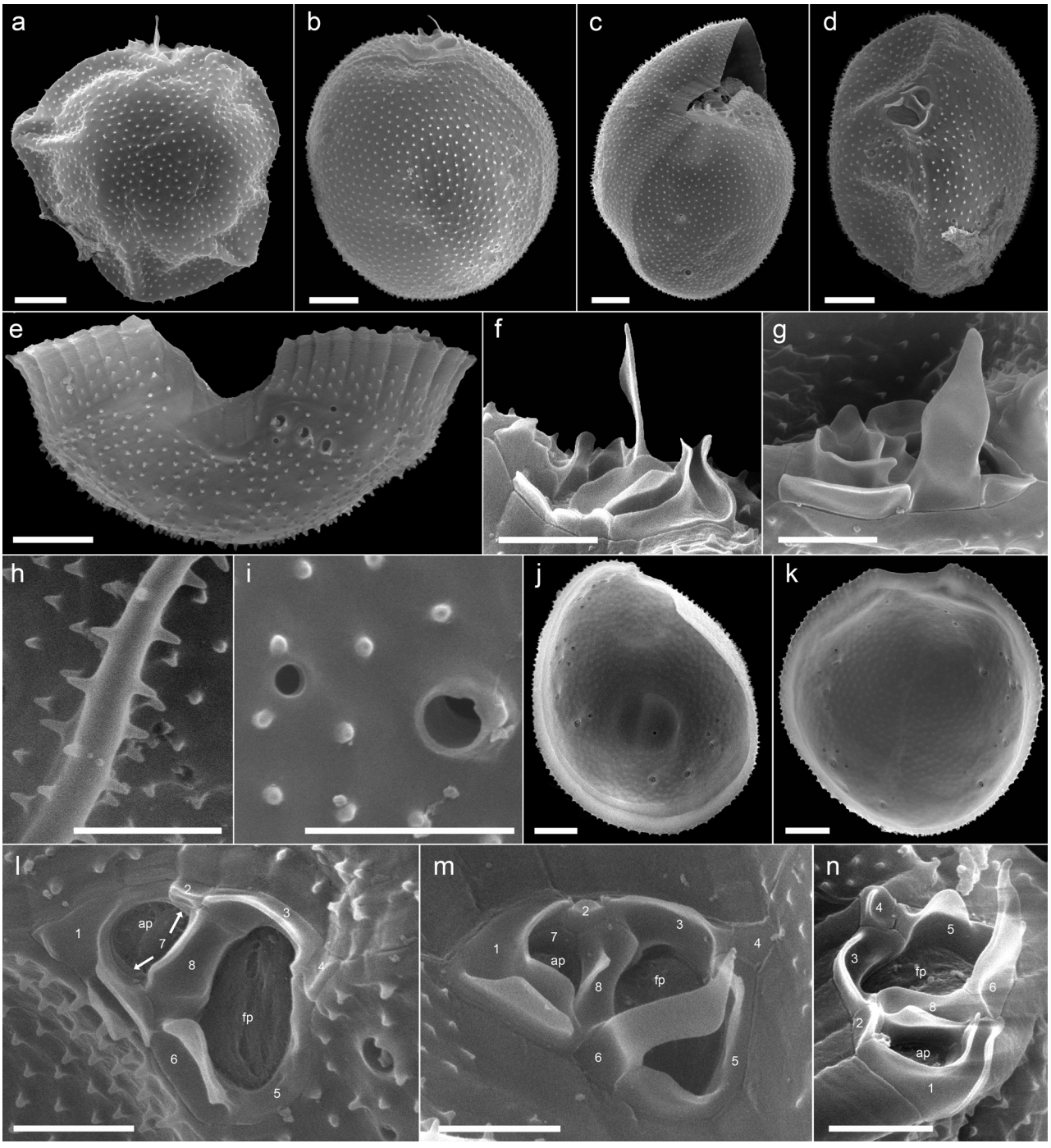

Fig. 3. *Prorocentrum pervagatum* sp. nov., strain PM-01. SEM of different thecate cells. (a–d) Right-lateral (a), left-lateral (b), dorsal-apical (c), or apical view (d). (e) Apical view of the right thecal plate. Note the broad and striated growth band close to the sagittal suture. (f, g) Detailed lateral view of the apical periflagellar area and the apical spine. (h, i) Detail of the surface ornamentation and the pores of two size classes. (j, k) Internal view of a thecal plate to indicate the position of thecal pores. (l–n) Detailed apical views of the periflagellar area. Numbers indicate denominations of periflagellar platelets, fp, flagellar pore; ap, accessory pore. Scale bars: 2 μm (a–e, j, k) and 1 μm (f–i, l–n).

Molecular phylogeny

A systematically representative set of prorocentralean and related accessions was compiled from known reference trees such as presented in Gottschling *et al*. (2020) and Tillmann *et al*. (2022). The taxon sample was enriched by all those accessions of small species of *Prorocentrum* deposited in GenBank, which comprise at least two of the three rRNA loci (i.e. SSU, ITS, LSU). Voucher information is provided in Table S1, which also includes GenBank accessions of *P. pervagatum* strains (OP094108–OP094113) and outgroup details comprising Dinophysales and Gymnodiniales. For alignment, separate matrices of the rRNA operon (i.e. SSU, ITS, LSU) were constructed, aligned using MAFFT v6.502a (Katoh & Standley 2013), and then concatenated. The aligned matrices are available as a file named 'pervagatum. nexus' upon request. Phylogenetic analyses were carried out using maximum likelihood (ML) and Bayesian approaches as described previously (Gottschling *et al*. 2020; Tillmann *et al*. 2022) using the resources available from the CIPRES Science Gateway (Miller *et al*. 2010). The clade containing sequences as assigned to *Prorocentrum shikokuense*, *P. donghaiense*, *P. obtusidens*, and *Prorocentrum dentatum* has been named the *P. dentatum* species complex based on the oldest name, because it is comprised of taxa, of which the identity and synonymy are still ambiguous (Shin *et al*. 2019; Gómez *et al*. 2021).

Terminology

Terminology of cell orientation and designation of thecal plates and platelets follow Hoppenrath *et al*. (2013) and include some additions and modifications as suggested by Tillmann *et al*. (2019).

RESULTS

Formal description

Prorocentrum pervagatum Tillmann, Hoppenrath & Gottschling, sp. nov. (Figs 2–5).

Description: Cells small, photosynthetic, thecate, asymmetrically oval to round in lateral view, 9–16 μm long and deep; cells moderately compressed laterally after division or almost round when old, then with a broad and transversely striated intercalary band; two reticulate chloroplasts, a round to oval nucleus in posterior position; presumable pusule in apical position, close to the flagellar pore. One small but distinct spine in apical position, of variable length. Periflagellar area composed of eight platelets (1 2 3 4 5 6 7 8), a small accessory pore, and a large flagellar pore, platelet 6 bearing the spine, other periflagellar platelets bearing flat lists. Both thecal plates densely covered by tiny cone-shaped to spine-like projections. Thecal pores (10–20 per plate) of two different size classes, scattered close to the plate margin; a short row of three to four large pores in apical-ventral position on the right thecal plate.

Holotype: SEM-stub prepared from monoclonal strain PM-01 (designated CEDiT**2022H145**), deposited at the Senckenberg Research Institute and Natural History Museum, Centre of Excellence for Dinophyte Taxonomy (Germany).

Isotype: Formalin-fixed sample prepared from clonal strain PM-01 (CEDiT**2022I146**), deposited at the Senckenberg Research Institute and Natural History Museum, Centre of Excellence for Dinophyte Taxonomy (Germany).

Type locality: North Atlantic, central Labrador Sea (56°49.42′ N; 52°13.15′ W).

Habitat: Marine water column.

Strain establishment: Sampled by U. Tillmann in June 2017, isolated by U. Tillmann in June 2017.

Etymology: The epithet (Lat. pervagatum – widely spread) reflects the very distant origin of strains established from Antarctic waters in the South, in subarctic waters in the North, and in temperate Atlantic waters.

This taxonomic act has been registered in PhycoBank (http://phycobank.org/103234).

Detailed description

All strains of *P. pervagatum* examined in the present study (Table 1) shared the same morphological features, despite regional differences in some morphometric details. Strain PM-01 from the central Labrador Sea was selected to prepare the type material of *P. pervagatum* and is depicted here in detail (Figs 2 and 3), together with material of field samples from the Labrador Sea (Fig. 4). Morphometric descriptions are based on all six strains established in the course of the present study, and micrographs of all other strains can be found in the Supporting Information (Figs S1–S9).

Light microscopy

Cells were asymmetrically oval to round in lateral view. Cell size ranged from 9.3 to 16.0 μm in length and depth with l/d ratios of close to 1 (Table 2). Cell width was difficult to measure but based on low-magnification observation of live and swimming/turning cells the length:width ratio was variable, ranging from 0.6 to 1, with almost globular cells dominating in dense cultures. In globose cells, a broad and densely striated growth band between both thecal plates was visible (Fig. 2j). A small but distinct spine was located at the cell's apex (Fig. 2f–h,k). The thecal surface appeared smooth, and thecal pores were difficult to detect in live or fixed cells in brightfield or differential interference contrast microscopy. However, pores were clearly observed on the surface of empty thecae (Fig. 2m) and in calcofluor-stained cells under UV excitation (Fig. 2k,l). Pores were located towards the thecal margins with a large central area on each theca devoid of pores.

Two yellow-orange and reticulate chloroplasts were arranged parietally and close to the thecal plates (Fig. 2c,i). In some cells, a small pyrenoid was faintly visible (Fig. 2e). A small, in outline round, hyaline pusule was occasionally present in the anterior area close to the flagellar pore (Fig. 2e). Long, rod-like structures (presumably trichocysts) were visible and mainly arranged along the cell's longitudinal axis (Fig. 2d). The large nucleus was oval to circular in outline and located in the posterior part of the cell (Fig. 2n–q). During cell division, the nucleus stretched along the longitudinal axis before division (elongated in ventral/dorsal view; Fig. S1n,o).

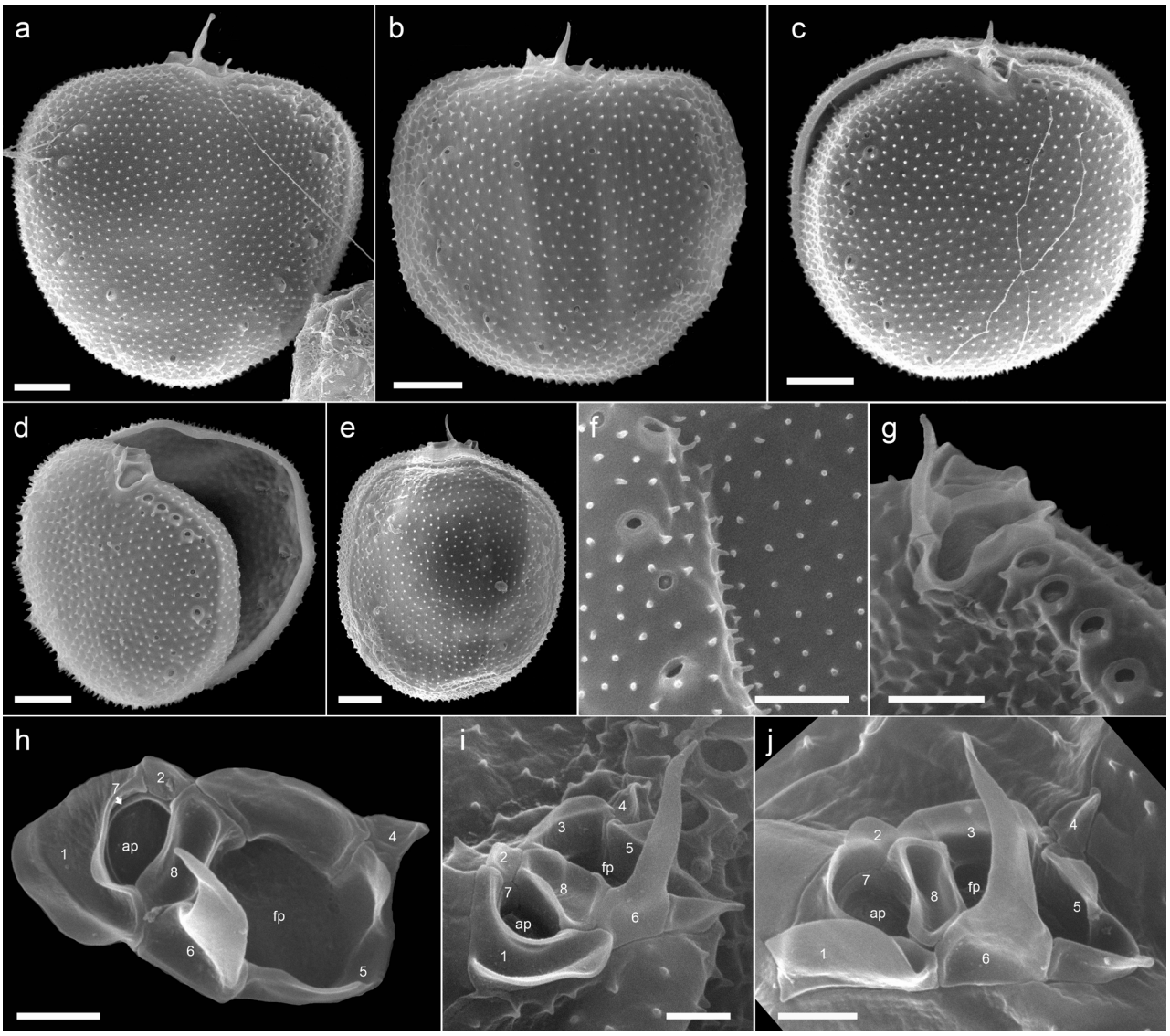

Fig. 4. *Prorocentrum pervagatum* sp. nov., field material from Station 1 in the central Labrador Sea. SEM of different thecate cells. (a–e) Right-lateral (a–c), right-lateral apical (d), or left-lateral view (e). (f) Surface structure of thecal plates. Note that the three-dimensional shape of the small knobs is visible in an artificially folded plate. Also note the presence of small and large thecal pores. (g) Ventral view of the apical periflagellar area. Note the row of four large thecal pores. (h–j) Detailed apical views of the periflagellar area. Numbers indicate denominations of periflagellar platelets; fp, flagellar pore; ap, accessory pore. Scale bars: 2 μm (a–e), 1 μm (f, g), and 0.5 μm (h–j).

One large flagellar pore and a distinctly smaller accessory pore in apical position could be adumbrated in regular LM (Fig. 2j) and were clearly visible in calcofluor-stained cells under UV excitation (Fig. 2l).

Scanning electron microscopy

The two large thecal plates were densely and uniformly covered by mainly knob-like to rarely spine-like, small projections (Figs 3 and 4). These projections were coniform in lateral view (Fig. 3h) and ranged in length from 0.13 to 0.25 μm. Mean projection length was slightly different between strains from different geographical origins and was smallest for the Antarctic strain (0.10 μm) and largest for the Labrador Sea material (0.17 μm) (Table 3). Mean areal density of projections was higher for strain CA-01 (10.5 μm^{-2}) compared to the Labrador Sea material (ranging from 7.0 to 7.5 μm^{-2}) and the North Sea strains (ranging from 7.5 to 8.5 μm^{-2}) (Table 3).

Thecal pores exhibited two size classes. Large pores were about 0.3 μm in diameter (Table 3) and delimited by a crateriform rim at the outer plate surface (Figs 3e,i and 4d,f,g), and had a slightly globular inward extension visible in internal plate views (Figs 3j,k; Fig. S2j). Small pores were about 0.15 μm in diameter (Table 3) and without any additional structure (Figs 3i–k and 4f; Fig. S2i,j). Three to four large pores were characteristically and linearly arranged on the right plate in apical ventral position (Figs 3d,e and 4c,d,g). Other pores were scattered on both thecal plates towards the plate

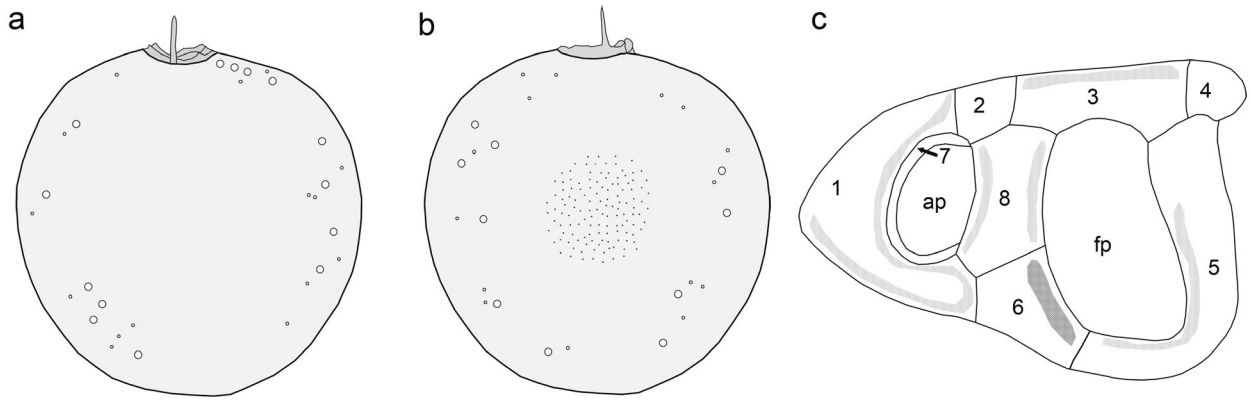

Fig. 5. *Prorocentrum pervagatum* sp. nov., schematic drawings of a representative pore pattern of the right (a) and left (b) theca. The density of thecal knobs is indicated in the center of the left plate in (b). (c) Schematic drawing of the periflagellar area. ap, accessory pore; fp, flagellar pore. Numbers indicate denominations of the platelets. Light gray indicates platelet lists; dark gray indicates apical spine.

margins (Figs 3b,c,j,k and 4a–d). The length of the apical spine ranged between 1.48 and 2.00 μm, with mean length for the North Sea strains (ranging from 1.11 to 1.23 μm) slightly lower compared those for the Antarctic strain (1.25 μm) and the Labrador Sea material (1.73 μm) (Table 2). The spine was 3–6 times as long as any other broad lists of the periflagellar platelets, which were 0.25–0.5 μm in height (Figs 3f,g and 4a,b,i,j). The small periflagellar area was 2.5 μm deep and 1.6 μm wide (Table 4) and located between both thecal plates in a broadly V-shaped indentation of the right plate (Figs 3e and 4d). There were eight platelets (1 2 3 4 5 6 7 8) surrounding a flagellar pore and an accessory pore (Figs 3l–n and 4h–j), with platelets 2 and 4 being strikingly small. The flagellar pore was of irregularly oval shape, generally longer than wide in right lateral through apical view (ca. 1.3 μm long, 0.7 μm wide, Table 4) and surrounded by platelets 3, 5, 6, and 8. The accessory pore was smaller (0.8 μm long, 0.5 μm wide, Table 4) and surrounded by platelets 7 and 8. Platelet 2 was part of the accessory pore's upper rim and separated by platelet 7 from the inner ring of the accessory pore (Figs 3l,m and 4h,j). Both pores were internally closed by two lip-like structures (Fig. 3l). Platelet 1 in dorsal position carried a characteristically winded, flat list bordering the accessory pore and forming a parallel double structure on the platelet's right side (Figs 3f,g, l–n and 4h–j) at the outer margin. The distinct spine was part of platelet 6 (Figs 3g,l–n and 4g–j). Platelet 4 was small, triangular, and plain and formed an acuminate ventral termination of the periflagellar area (Figs 3l–n and 4h–j). All other platelets had short and irregular platelet lists (Figs 3f,g,l–n and 4h–j). Occasionally, a large, pore-like depression was observed on the upper ventral corner of platelet 5 (Figs S3b–d and S7f).

A schematic drawing of the new species including a representative pore pattern and a schematic drawing of the periflagellar area is presented in Figure 5.

Molecular phylogenetics

The SSU + ITS + LSU alignment was 1797 + 746 + 3484 bp long and composed of 302 + 525 + 835 parsimony-informative sites (28%, mean of 14.84 per terminal taxon) and 2774 distinct RAxML alignment patterns. Figure 6 shows the best-scoring ML tree (−ln = 55 051.96, being highly similar to the Bayesian tree), with the internal topology not fully resolved. With respect to Dinophysales and Gymnodiniales, three lineages, including

Table 2. *Prorocentrum pervagatum* sp. nov.: Morphometry, cell size measurements. nd = not determined

Origin	Strain	Cell length (μm) mean ± SD min–max	Cell depth (μm) mean ± SD min–max	l/d ratio mean ± SD	*N*	Spine length (μm) mean ± SD min–max	*N*
Antarctica	CA-01	13.9 ± 0.8 12.0–15.7	14.6 ± 0.6 13.5–15.6	0.98 ± 0.02	53	1.25 ± 0.11 1.04–1.49	26
Norway	P3-B7	11.5 ± 1.1 9.5–14.3	11.2 ± 1.1 9.0–13.7	1.03 ± 0.07	54	1.11 ± 0.17 0.87–1.43	15
Norway	P3-C7	10.6 ± 1.3 8.3–15.2	10.2 ± 1.2 8.0–14.2	1.04 ± 0.06	75	1.23 ± 0.18 0.90–1.49	15
Labrador Sea	PM-01	13.6 ± 1.0 11.4–16.0	13.1 ± 1.2 9.3–15.9	1.04 ± 0.06	62	1.70 ± 0.16 1.48–2.00	12
Labrador Sea	Field sample LS	nd	nd	nd		1.73 ± 0.23 1.41–2.17	10
German Bight	LP-D3	12.1 ± 1.2 10.0–14.7	11.2 ± 1.2 9.2–14.3	1.05 ± 0.05	56	1.20 ± 0.13 1.02–1.45	17
German Bight	LP-D10	11.7 ± 1.2 9.2–14.3	10.6 ± 1.3 8.2–13.7	1.08 ± 0.06	48	1.16 ± 0.10 1.01–1.43	14

Table 3. *Prorocentrum pervagatum* sp. nov.: Morphometry of projections and pores

Origin	Strain	Thecal plate projections		Pore size (μm)		Number of pores			
		Length (μm)	Density (μm^{-2})	Large	Small	Right plate		Left plate	
		mean ± SD min–max	mean ± SD min–max	mean ± SD min–max	mean ± SD min–max	Large	Small	Large	Small
Antarctica	CA-01	0.10 ± 0.01 0.08–0.12 *n* = 12	10.5 ± 1.0 8.8–12.7 *n* = 42	0.34 ± 0.03 0.26–0.40 *n* = 35	0.16 ± 0.01 0.13–0.19 *n* = 45	11.5 ± 1.0 10–13 *n* = 17	15.4 ± 3.1 11–24 *n* = 17	10.0 ± 1.1 8–12 *n* = 11	15.4 ± 2.4 11–20 *n* = 11
Norway	P3-B7	0.12 ± 0.02 0.09–0.15 *n* = 27	8.2 ± 0.8 6.3–10.0 *n* = 20	0.29 ± 0.03 0.22–0.37 *n* = 20	0.15 ± 0.01 0.12–0.17 *n* = 20	7.8 ± 1.6 6–10 *n* = 11	11.8 ± 1.2 10–14 *n* = 11	6.8 ± 0.1.8 4–10 *n* = 13	11.2 ± 2.6 6–15 *n* = 13
Norway	P3-C7	0.12 ± 0.02 0.09–0.15 *n* = 25	8.5 ± 0.6 7.1–10.3 *n* = 20	0.25 ± 0.03 0.20–0.33 *n* = 23	0.14 ± 0.01 0.11–0.17 *n* = 33	n.d.	n.d.	n.d.	n.d.
Labrador Sea	PM-01	0.16 ± 0.02 0.13–0.25 *n* = 26	7.0 ± 0.4 6.1–7.8 *n* = 21	0.31 ± 0.02 0.29–0.34 *n* = 9	0.15 ± 0.01 0.14–0.16 *n* = 10	9.6 ± 1.3 7–12 *n* = 11	15.6 ± 3.1 10–21 *n* = 11	9.3 ± 1.5 8–12 *n* = 9	14.2 ± 2.6 10–19 *n* = 9
Labrador Sea	Field sample LS	0.17 ± 0.02 0.14–0.24 *n* = 33	7.5 ± 0.4 6.9–8.1 *n* = 21	0.28 ± 0.05 0.17–0.37 *n* = 37	0.16 ± 0.01 0.14–0.18 *n* = 17	11.7 ± 1.1 10–14 *n* = 10	16.7 ± 2.7 12–23 *n* = 10	8.4 ± 0.8 7–9 *n* = 5	14.6 ± 2.6 11–19 *n* = 5
German Bight	LP-D3	0.11 ± 0.02 0.08–0.14 *n* = 32	7.7 ± 0.6 6.8–9.2 *n* = 20	0.26 ± 0.03 0.20–0.32 *n* = 26	0.14 ± 0.01 0.12–0.17 *n* = 29	7.3 ± 1.1 6–10 *n* = 14	18.9 ± 2.6 13–23 *n* = 14	6.3 ± 1.0 4–8 *n* = 15	19.6 ± 2.9 15–25 *n* = 15
German Bight	LP-D10	0.11 ± 0.02 0.07–0.14 *n* = 32	7.5 ± 0.5 6.4–8.8 *n* = 20	0.26 ± 0.03 0.21–0.32 *n* = 29	0.14 ± 0.02 0.11–0.17 *n* = 31	7.8 ± 1.3 5–10 *n* = 9	18.2 ± 2.7 15–22 *n* = 9	6.6 ± 1.5 4–9 *n* = 12	19.0 ± 3.5 14–25 *n* = 12

Adenoides Balech (98LBS, 1.00BPP), *Plagiodinium* M.A.Faust & Balech (100LBS, 1.00BPP), and *Prorocentrum*, formed a well-supported clade (83LBS, 1.00BPP). *Prorocentrum* was comprised of two clades, denominated here PRO1, including the type species *P. micans* (100LBS, 1.00BPP), and PRO2 (96LBS, 1.00BPP).

The PRO1 clade consisted of five well-supported lineages, two of which were comprised of benthic species such as *Prorocentrum tsawwassenense* Hoppenrath & B.S.Leander (95LBS, 1.00BPP) and *Prorocentrum fukuyoi* Sh.Murray & Nagahama (92LBS, 1.00BPP), respectively. The third lineage constituted the *P. micans* species complex (66LBS,

Table 4. *Prorocentrum pervagatum* sp. nov.: Periflagellar area sizes

Origin	Strain	Periflagellar area		Size accessory pore		Size flagellar pore	
		Depth (μm)	Width (μm)	Length (μm)	Width (μm)	Length (μm)	Width (μm)
		mean ± SD min–max	mean ± SD min–max	mean ± SD min–max	mean ± SD min–max	mean ± SD min–max	mean ± SD min–max
Antarctica	CA-01	2.7 ± 0.2 2.4–3.0 *n* = 15	1.8 ± 0.1 1.5–1.9 *n* = 15	0.8 ± 0.1 0.6–0.8 *n* = 15	0.5 ± 0.1 0.4–0.6 *n* = 15	1.5 ± 0.1 1.2–1.7 *n* = 15	0.8 ± 0.1 0.7–1.0 *n* = 15
Norway	P3-B7	2.3 ± 0.1 2.1–2.5 *n* = 7	1.6 ± 0.1 1.5–1.7 *n* = 7	0.8 ± 0.1 0.7–0.9 *n* = 7	0.5 ± 0.1 0.4–0.5 *n* = 7	1.3 ± 0.1 1.2–1.4 *n* = 7	0.7 ± 0.1 0.7–0.8 *n* = 7
Norway	P4-C7	2.2 ± 0.1 1.9–2.3 *n* = 11	1.4 ± 0.1 1.2–1.7 *n* = 11	0.7 ± 0.1 0.6–0.8 *n* = 11	0.4 ± 0.1 0.4–0.5 *n* = 11	1.2 ± 0.1 1.0–1.4 *n* = 11	0.6 ± 0.1 0.5–0.8 *n* = 11
Labrador Sea	PM-01	2.5 ± 0.3 2.0–3.3 *n* = 15	1.6 ± 0.2 1.3–1.9 *n* = 15	0.8 ± 0.1 0.7–1.1 *n* = 15	0.5 ± 0.1 0.4–0.6 *n* = 15	1.3 ± 0.1 1.1–1.5 *n* = 15	0.7 ± 0.1 0.6–0.9 *n* = 15
Labrador Sea	Field sample LS	2.6 ± 0.2 1.7–2.6 *n* = 9	1.3 ± 0.1 1.1–1.5 *n* = 9	0.6 ± 0.1 0.5–0.7 *n* = 7	0.5 ± 0.1 0.4–0.6 *n* = 7	1.1 ± 0.1 0.8–1.2 *n* = 7	0.7 ± 0.1 0.6–0.8 *n* = 7
German Bight	LP-D3	2.7 ± 0.2 2.4–3.0 *n* = 8	1.6 ± 0.1 1.4–1.7 *n* = 8	0.9 ± 0.1 0.8–0.9 *n* = 8	0.6 ± 0.1 0.5–0.64 *n* = 8	1.3 ± 0.1 1.1–1.5 *n* = 8	0.7 ± 0.1 0.6–1.0 *n* = 8
German Bight	LP-D10	2.9 ± 0.2 2.5–3.1 *n* = 4	1.6 ± 0.1 1.4–1.7 *n* = 4	0.9 ± 0.0 0.8–0.9 *n* = 4	0.6 ± 0.0 0.6–0.7 *n* = 4	1.4 ± 0.1 1.2–1.5 *n* = 4	0.7 ± 0.1 0.7–0.8 *n* = 4

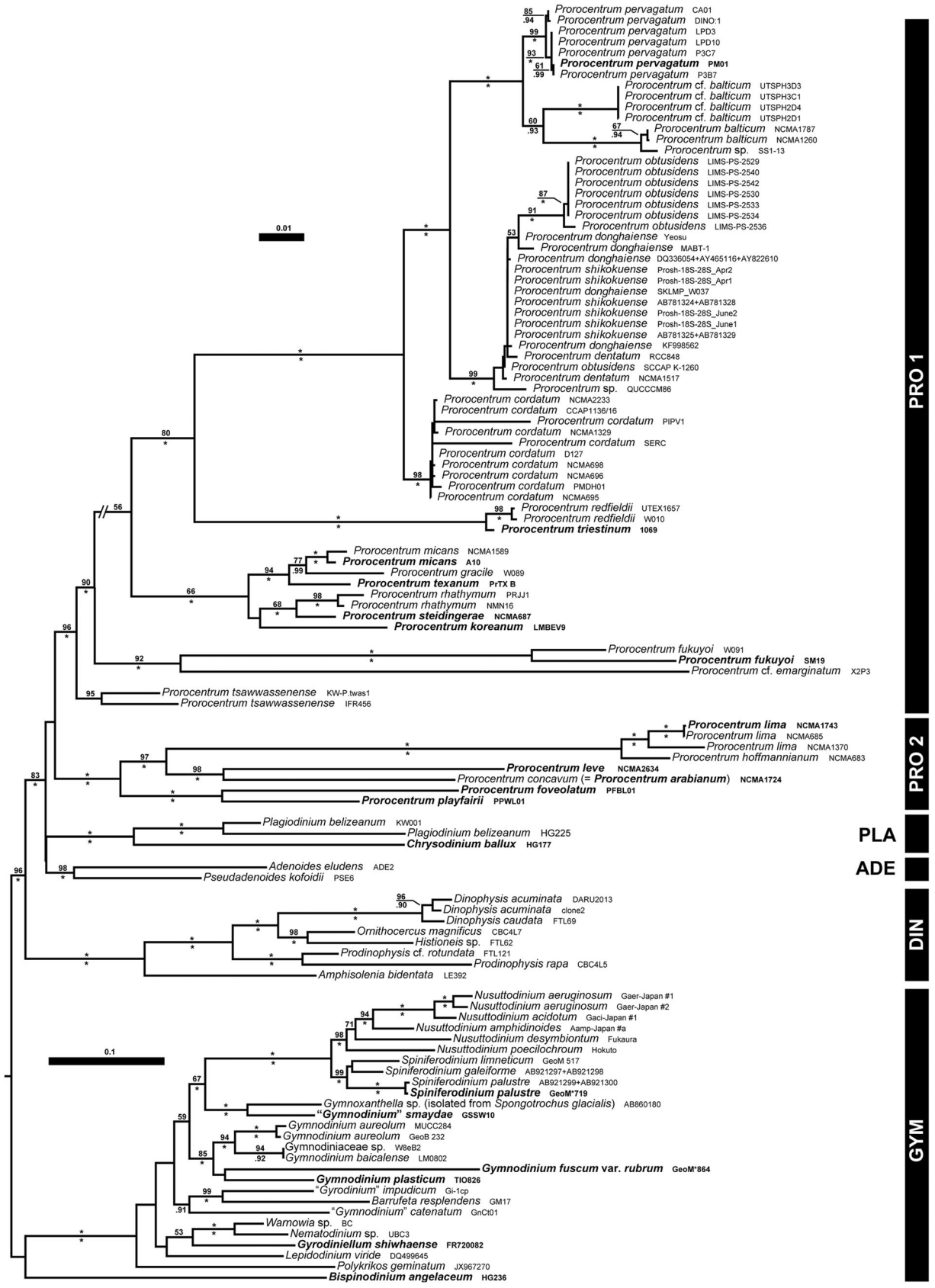

Fig. 6. Legend on next page.

1.00BPP), whereas the fourth lineage included accessions of *P. triestinum* J.Schiller and relatives (100LBS, 1.00BPP). The fifth lineage (100LBS, 1.00BPP) included all accessions investigated in the present study, together with *P. balticum*, *P. cordatum*, and taxa of the *P. dentatum* species complex. As inferred from short branches, sequence divergence was low within *P. pervagatum* (100LBS, 1.00BPP), which constituted the sister group (100LBS, 1.00BPP) of *P. balticum* (60LBS, 0.93BPP). Within the *P. pervagatum* clade three ribotypes could be detected differing in two or four positions of the ITS and LSU, respectively. Sequences for one published *Prorocentrum* sp. (strain DINO:1) belonged to *P. pervagatum*.

DISCUSSION

The taxonomy of small (i.e. <20 μm in length) species of *Prorocentrum* with a round outline by LM is challenging. The application of scientific names is frequently ambiguous if type material consists of drawings only. DNA sequence information is crucial for reliable determination particularly of minute protist species (Kretschmann *et al*. 2018a; Žerdoner Čalasan *et al*. 2020; Tillmann *et al*. 2022) and must be complemented with the demonstration of subtle morphological features such as the presence/absence of apical projections, plate surface structure (thecal ornamentation), and the presence and location of thecal pores. Among the 14 described species of *Prorocentrum* in this size class (Table 5, Fig. 7), there are only two (i.e. *P. nux* and *P. ponticum*) with type material having been studied by EM (Puigserver & Zingone 2002; Krakhmalny & Terenko 2004). Moreover, DNA sequence data linked to original material are available for none of the small species. As result, taxonomists and users are left with some basic morphological features such as size and shape and a rather classical evaluation on the nature of apical extensions. However, the morphological details described in the protologues of species smaller than 20 μm (Table 5) allow for a robust diagnosis of *P. pervagatum*. A number of scientific names are currently sunk in synonymy (Dodge 1975) but due to significant differences in traits such as size, the corresponding taxa are included in the diagnosis as well and discussed here.

A widespread and probably the most intensely studied small species of *Prorocentrum* is known as *P. cordatum* from the Caspian Sea, which the majority of authors currently synonymize with *P. minimum* from the Mediterranean Sea (as firstly proposed by Velikova & Larsen 1999). Nevertheless, *P. cordatum* has been described by Ostenfeld (1902) to lack an apical spine or other apical projections (Fig. 7a), whereas a 'small tooth with minute wing' is clearly present in *P. minimum* (Pavillard 1916; Schiller 1933) (Fig. 7b). Synonymization is based on studies of specimens from the Caspian Sea, which have always shown the apical appearance of true *P. minimum* (Velikova & Larsen 1999), and the same refers to further analyses of small specimens of *Prorocentrum* from the Azov Sea (a northern marginal sea of the Black Sea) (Krakhmalny *et al*. 2004). EM of *P. minimum* shows complex apical projections, which are better described by a distinct double wing on platelet 1 (which correspond to the spine as described based on LM) and additional extensions on other platelets (Pertola *et al*. 2003; Monti *et al*. 2010). This clearly illustrates the difficulties to evaluate apical structures in historical descriptions of *Prorocentrum*, and we therefore follow Velikova and Larsen (1999), assuming that both names *P. cordatum* and *P. minimum* refer to the same species, with *P. cordatum* having priority. A number of presumed synonyms of *P. cordatum* (or *P. minimum*) are listed in the literature [*Exuviaella pacifica* Kuzmina, *P. cordiforme* Bursa, *nom. corr.*: ICN Art. 23.5, *P. marielebouriae* (Parke & Ballentine) A.R.Loeblich, *Prorocentrum pyriforme* (J.Schiller) Hasle ex F.J.R.Taylor, *P. triangulatum* G.W.Martin, and also freshwater *Exuviaella peisonis* J.Schiller], but future studies of material from the respective type localities are required to unambiguously clarify the taxonomic status of taxa in this species complex. In any case, *P. cordatum* and putatively related species are different from *P. pervagatum*, because of the thecal pore pattern, details of the spiny ornamentation, and the distinct lateral compression of *P. cordatum*, among others (Table 5).

Prorocentrum balticum described by Lohmann (1908) from Kiel (German Baltic Sea) (Fig. 7c) is another frequently encountered small species of *Prorocentrum* (Faust *et al*. 1999; Larsen & Nguyen-Ngoc 2004; Hoppenrath *et al*. 2009). Whether such determinations in fact represent the organism described by Lohmann (1908) is questionable considering the gross similarity of the small species. As usual for the time of description, the protologue provides a few basic features only, such as the small size (9–12 μm), the shape (slightly ovoid in lateral view, almost round in ventral view), and the visible sagittal suture. The original description is silent about the presence or absence of an apical spine or other obvious apical projections, but Lohmann (1908) briefly mentions a colorless plasma plug in apical position that he observed a few times. Moreover, pores or other surface features of the thecal plates are not reported in the protologue. The descriptions of subsequent authors deviate from this information in cells having two minuscule teeth (Wulff 1916: '*zwei winzige Zähnchen*', though hardly visible in the accurate drawing) in the apical area or having a single, flat, and triangular fin located orthogonally to both apical pores (Adachi 1972) or having two distinct apical spines (Steidinger & Tangen 1996). In any case, true *P. balticum* can be differentiated from *P. pervagatum* by the lack of an apical spine, as long as the plasma plug occasionally observed (Lohmann 1908) does not turn out a spiny apical projection. In the molecular phylogenetic tree, *P. pervagatum* is the sister lineage of strains determined as *P. balticum* (CCMP1787 from the South Pacific and CCMP1260 from the Gulf of Mexico) or

Fig. 6. Molecular phylogenetics of Prorocentrales, including all seven accessions assignable to *Prorocentrum pervagatum* sp. nov. ML tree (−ln = 55 051.96), as inferred from an rRNA nucleotide alignment (1662 parsimony-informative sites) with strain number information. Accessions corresponding to type or at least reference material are shown in bold type, freshwater accessions are shown in gray, and strains sequenced in this study are shown in red. Numbers on branches are ML bootstrap (above) and Bayesian support values (below) for the clusters (asterisks indicate maximal support values; values under 50 and 0.90, respectively, are not shown). Clades are indicated (abbreviations: ADE, *Adenoides*; DIN, Dinophysales; GYM, Gymnodiniales; PLA, *Plagiodinium*; PRO, *Prorocentrum*).

Table 5. Comparison of small *Prorocentrum* species

feature	*P. pervagatum* sp. nov.	*P. cordatum** Ostenfeld	*P. balticum* Lohmann	*P. sphaeroideum* J.Schiller†	*P. nux* Puigserver & Zingone	*P. nanum* J.Schiller	*P. ovum* J.Schiller	*P. pusillum*‡ J.Schiller§	*P. rotundatum* J.Schiller	*P. antarcticum* ** (Hada) Balech	*P. ponticum* Krakhmalny & Terenko	*P. cornutum* J.Schiller	*„E". equatorialis* Hasle††	*P. pomoideum* Bursa‡‡	*P. cordiforme* Bursa§§
shape	rounded	obcordate emarginate heart-shaped	rounded ovate	round	irregularly oval	irregular, almost angular contour lines	ovate, anterior end square***	ovate	almost round to oval	ovate large oval to almost pentagonal	orbicular to broadly elliptic	curved contour lines, with a posterior horn-like pointed end	almost circular	apple shaped (often with posterior constriction)	heart-shaped
length	12-16	22–24 µm 18 µm	9–12 µm	13 µm	6.3–9 µm	10–14 µm	14 µm	8–10 µm	16–21 µm	15-17 µm 20–23 µm	10.4–15.1	16 µm	19 µm	9–20 µm	6–12 µm
depth	12-16	18–20 µm 15 µm	9–12 µm	13 µm	5.3–10 µm	10–14 µm	10 µm	6.5–7.5 µm	16–24 µm	12-15 µm 17.5–19.5	9.6–11.5	14 µm	19 µm	11–16 µm	5–9 µm
compression	young cells slightly compressed; round	compressed strongly compressed	round		5.3–10.7 µm	strongly compressed	scarcely compressed	strongly compressed	slightly compressed	fairly compressed laterally compressed	slightly or strongly compressed	not mentioned	elliptical, markedly compressed	flattened	not reported
apical spine	yes 1.3–1.7 µm, on platelet 6	no small tooth with minute wing	no	yes a solid spine without wing	no	yes short spine†††	no	no	yes solid spine with a membrane	no no	no	yes a delicate thin tooth with a hyaline wing	no	yes one main apical tooth without a wing	short simple spine‡‡‡
projections	flat wings	no no	not reported		no	two irregular bumps bordering the flagellar pore	no	no	an uneven bump between pore and spine	no no	small projections	an insignificant indentation next to the flagellar pore	a small projecting flange between the two apical pores	two more and smaller "spines"	one additional smaller spine opposite to the other spine
surface	knobs	with fine pores§§§ very densely perforated with subtle pores****	not reported	not described	smooth	not described	not described	with subtle pores††††	not described	smooth, minute perforation hardly visible not described	knobs	not described	„with spines (pores?)."	spines / smooth‡‡‡‡	smooth
pores	yes	not reported not reported	not reported	yes	yes	yes	yes	yes	not specified	no pores few minute scattered pores	one line of fine pores located on the periphery of each thecal plate	not described	not described	numerous small pores	no traces of pores§§§§
pore size	large (0.3 µm) small (0.16 µm)	not reported not reported	not reported	large	large and small	large	large	subtle	not specified	no pores minute	fine pores	not described	not described	small	no pores observed
pore number	ca. 20–30 per plate	not reported not reported	not reported	few	few	scarce	few	not specified or drawn	not specified	no pores few	??	not described	not described	numerous	no pores observed
pore position	scattered on the plate margin	not reported not reported	not reported	all over the thecae	close to plate margins	scattered all over the theca	scatted all over the theca	not specified	not specified	no pores Scattered	arranged in one line on the periphery of each thecal plate	not described	not described	scattered all over the theca	no pores observed
type locality	Labrador Sea	Caspian Sea Golfe de Lion, France	Kiel Bight, Baltic Sea	Adriatic Sea	Tyrrhenian Sea, off Naples	Adriatic Sea	Adriatic Sea	Adriatic Sea	Adriatic Sea	Lützow-Holm Bay, eastern Antarctica	Black Sea	Adriatic Sea	Tropical Pacific	Yamar estuary	Plymouth
distribution	Antarctica, Labrador Sea, North Sea	Caspian Sea Mediterranean	Baltic Sea (Kiel)	Mediterranean	Tyrrhenia Sea, English channel	Adriatic Sea, North Sea, Atlantic	Adriatic Sea	Adriatic Sea	Adriatic Sea, Tyrrhenian Sea	Antarctica	Black Sea	Mediterranean	Tropical Pacific	Yamar estuary	Plymouth
periflagellar platelets	8	- *****	-	-	7	-	-	-	-	-	-	-	-	-	-
references	this study	Ostenfeld 1902 Schiller 1933	Lohman 1908	Schiller 1918	Puigserver & Zingone 2002	Schiller 1918	Schiller 1918	Schiller 1928	Schiller 1918	Hada 1970 Balech 1976	Krakhmalny & Terenko 2004	Schiller 1918	Hasle 1960	Bursa 1959	Bursa 1959

*Descriptions of both C.H. Ostenfeld (in white) for *P. cordatum* and J. Schiller (in gray) for *P. minimum* are given. †Dodge (1975) considered this species a synonym of *P. scutellum*. ‡It is important to note that the taxon analyzed by Dodge & Bibby (1973) and Dodge (1975) under the name *P. pusillum* later turned out to be *P. nux* (see Puigserver & Zingone 2002). §Dodge (1975) considered this species a synonym of *P. nanum*. **Descriptions of both Y. Hada (in white) and E. Balech (in gray) are given. ††Dodge (1975) considered this species a synonym of *P. balticum*. ‡‡Dodge (1975) considered this species a synonym of *P. balticum*. §§Dodge (1975) considered this species a synonym of *P. minimum*. ***In J. Schiller's drawing and description, the flagella emerge from a deeply indented apical area formed by one of the thecal plates. This would make *P. ovum* distinct from all other small, roundish species of *Prorocentrum*. †††The protologue reads: 'Almost always one short spine on one of the bumps'. However, no 'spine' is visible in J. Schiller's drawing. ‡‡‡The height of the spine is reported as 1.5–2 µm. §§§According to C.H. Ostenfeld's drawing showing numerous mini-dots on the surface, these are spines and not pores. ****According to the original drawing from J. Pavillard reproduced by J. Schiller, but these mini-dots are spines rather than pores. ††††It is not clear if the 'subtle pores' described by J. Schiller in fact are pores or are indicative of a spiny or knobby plate surface structure. ‡‡‡‡The original description of A.S. Bursa reads: 'some individuals are covered with tiny spines, others are smooth'. §§§§Though three to six rod-shaped trichocysts are present inside the cells. *****Periflagellar platelet number of *P. minimum* is reported as eight in subsequent papers (Loeblich 1976; Taylor 1980; Honsell & Talarico 1985).

P. cf. *balticum* (from Australia). However, for none of these strains there is a sound morphological characterization, making it impossible to evaluate if they are true *P. balticum*. The re-investigation of *P. balticum* from the type locality at Kiel using contemporary morphological and molecular methods would resolve such doubts, but repeated sampling in the Kiel Bight during the past years did not yet succeed in obtaining cells conforming with H. Lohmann's protologue.

Similarly to the *P. cordatum* species complex, some synonyms of *P. balticum* are considered (Dodge 1975), such as *E. aequatorialis* and *P. pomoideum*. However, such synonymization is questionable since both such taxa are markedly compressed and are, therefore, both different from *P. pervagatum* (listed as a distinct species in Table 5). Moreover, *P. pomoideum* (Fig. 7d) has distinct structures (unclear whether pores or spines) on the plate surface and is different from *P. pervagatum* (and *P. balticum* as well) also in this respect. *Exuviaella aequatorialis* (Fig. 7e) is a small species from the tropical Pacific (Hasle 1960). However, it is significantly larger than *P. pervagatum* and has no apical spine. *Exuviaella aequatorialis* has been also synonymized with *Prorocentrum lenticulatum* (Matzenauer) F.J.R.Taylor (Gómez *et al*. 2008), but this is questionable as well because *P. lenticulatum* is significantly larger [cell length of 36 μm in Matzenauer (1933), 30–39 μm in Taylor (1976), compared to 19 μm provided in the protologue for *E. aequatorialis* in Hasle (1960)].

A total of six small species of *Prorocentrum* are described from the Adriatic Sea, a part of the Mediterranean Sea (Schiller 1918, 1928). These are listed in the following. (1) *Prorocentrum sphaeroideum* (Fig. 7f) resembles *P. pervagatum* in shape and presence of an apical spine, but it is slightly smaller (cell length of 9–12 μm in length for *P. sphaeroideum* vs. 12–16 μm for *P. pervagatum*). Most significantly, *P. sphaeroideum* has thecal pores evenly distributed on the thecal plates, whereas pores of *P. pervagatum* are only present close to the plate margins. Together with *Prorocentrum robustum* B.F.Osorio, *P. sphaeroideum* was put into synonymy of *Prorocentrum scutellum* Schröder (Dodge 1975), but these two alternate names represent species being much larger [*P. scutellum*: 45 μm in length, Schröder (1900); *P. robustum*: 36–43 μm in length, Osorio-Tafall (1942)] and thus different from *P. sphaeroideum*. (2) *Prorocentrum nanum* (Fig. 7g) is also small (10–14 μm in length), but this species has a strong lateral cell compression and thus can be differentiated from *P. pervagatum*. Moreover, *P. nanum* has thecal pores evenly scattered over the entirety of thecal plates (Schiller 1918), again different from *P. pervagatum* having pores close to the plate margins only. (3) *Prorocentrum pusillum* (Fig. 7h) has been considered a variation of *P. nanum* with thin cell walls (Dodge 1975). However, even the little information provided in the original description allows for a clear differentiation between *P. nanum* and *P. pusillum* primarily based on the cells' outline and the number, size, and position of thecal pores (Puigserver & Zingone 2002). Furthermore, a short apical spine is present in *P. nanum*, whereas *P. pusillum* lacks an apical spine. With the latter trait, *P. pusillum* can be differentiated from *P. pervagatum*. (4) The ovate cell shape of *P. ovum* in outline, with a square anterior end (Fig. 7i), differs from the asymmetrically oval to round shape of *P. pervagatum* in lateral view. Furthermore, this species has a very peculiar wedged depression at the flagella insertion, and thecal plates are interspersed with irregularly arranged pores, making it impossible to confuse *P. ovum* with *P. pervagatum*. (5) *Prorocentrum rotundatum* (Fig. 7j) is a poorly known species without description of the thecal plates' structure or of the presence/absence/arrangement of thecal pores. The species has a solid spine, but it differs significantly from *P. pervagatum* by its larger size (16–24 μm in length). (6) *Prorocentrum cornutum* (Fig. 7k) is exceptionally easy to differentiate from all other small species of *Prorocentrum* because of its very conspicuous shape exhibiting an asymmetric and horn-like posterior extension.

Another small species of *Prorocentrum*, Atlantic *P. cordiforme* (Fig. 7l) (Bursa 1959), is widely considered a junior synonym of *P. cordatum* (= *P. minimum*) (Dodge 1975). However, the heart-shaped cell and the much smaller size (6–12 μm in length) are very different from *P. pervagatum* (and from both *P. cordatum* and *P. minimum* as well). An additional, striking feature of *P. cordiforme* is a central (stalked) pyrenoid with starch sheath easily visible in LM (Bursa 1959) that is absent from all other small species of *Prorocentrum* discussed here.

Prorocentrum antarcticum (Fig. 7m,n) originates from Antarctic waters, more specifically from an area close to King George Island, from where strain CA-01 of *P. pervagatum* has been isolated. Notably, the original description of Hada (1970) (Fig. 7m) differs in size from that of Balech (1976) (Fig. 7n), who taxonomically transferred the species to *Prorocentrum*. Moreover, the thecal surface is smooth in Hada (1970) but scattered with pores in Balech (1976). In any case, both descriptions differ significantly from *P. pervagatum* by their strong lateral compression and by the absence of apical extensions and/or spines.

One of the more recently described small species of *Prorocentrum* is *P. nux* (Puigserver & Zingone 2002) (Fig. 7o) from the Mediterranean. It cannot be confused with *P. pervagatum* because of its very small size and by the smooth thecal surface. It was described with only seven periflagellar platelets (compared to eight platelets in *P. pervagatum*), but it is difficult to evaluate if the small and laboriously observable platelet 7 is indeed missing in *P. nux* or just has been overlooked.

Prorocentrum ponticum (Fig. 7p) from the northwestern Black Sea (Krakhmalny & Terenko 2004) shares some features with *P. pervagatum*, such as a similar size and thecal pores scattered along the plate margins. However, *P. ponticum* can be strongly compressed, it has only flat lists but no apical extensions and/or spines, and its plate surface ornamentation is characterized by thicker, round knobs (Krakhmalny & Terenko 2004) than in *P. pervagatum*.

Showing minor sequence variability, *P. pervagatum* is clearly separated from its close relatives (Fig. 6). Published sequences of an Antarctic *Prorocentrum* species of unknown identity (Bolinesi *et al*. 2020) also belong to *P. pervagatum*. Interestingly, it clustered closely together with the Antarctic strain of this study, suggesting regional ribotypes. Its morphology has not been presented and thus cannot be discussed in this context. The most closely related taxa included in the phylogenetic analyses (the fifth lineage comprising *P. balticum*, *P. cordatum*, and the *Prorocentrum dentatum* species complex) are similar in their thecal ornamentation (densely covered with spines or knobs) and their relatively small cell size, but more morphological and molecular data of small planktonic *Prorocentrum* species including

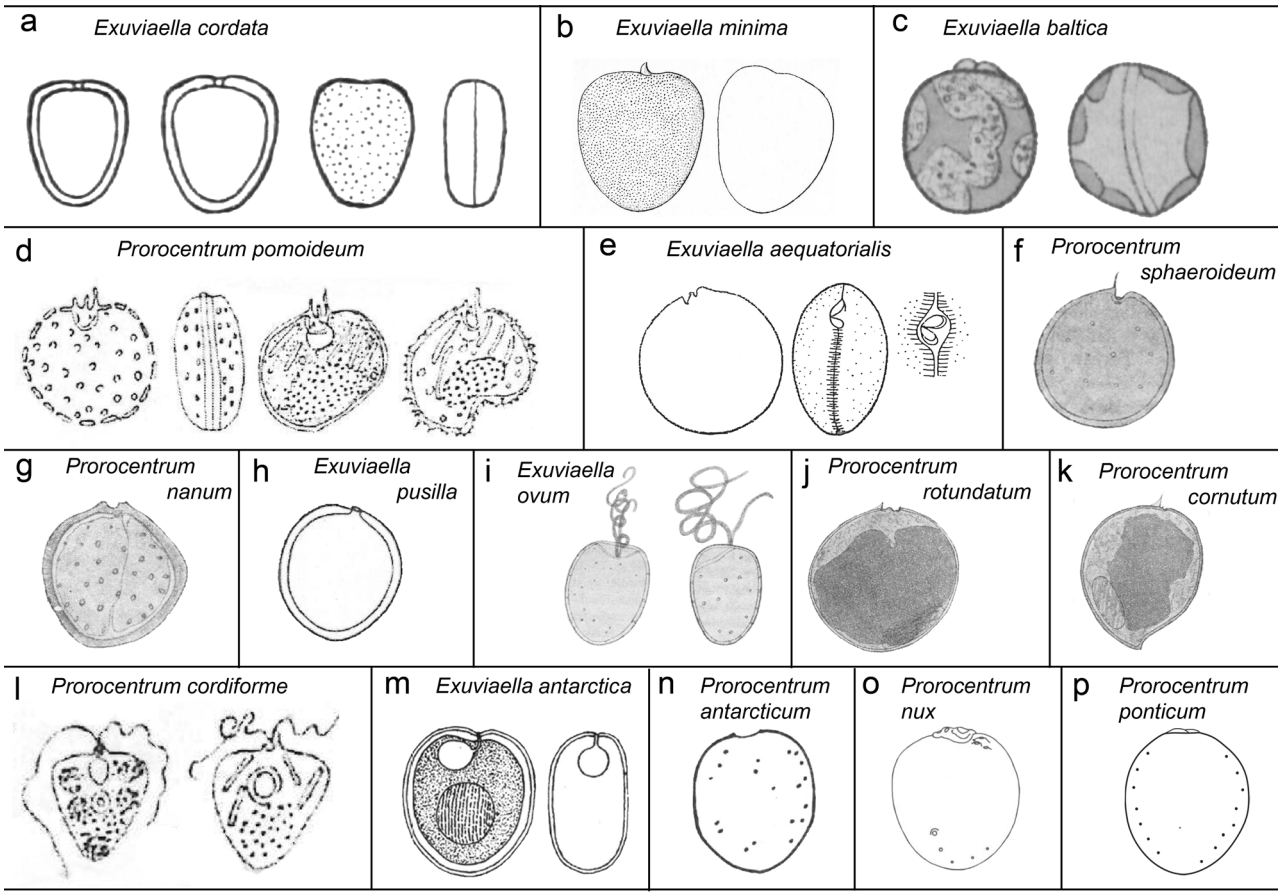

Fig. 7. Line drawings of small species assigned to *Prorocentrum* from the protologues (if they have been described under *Exuviaella*, then the basionym is used in the figure). (a) *Prorocentrum cordatum* (redrawn after Ostenfeld 1902). (b) *Prorocentrum minimum* (redrawn after Pavillard 1916). (c) *Prorocentrum balticum* (redrawn after Lohmann 1908). (d) *Prorocentrum pomoideum* (redrawn after Bursa 1959). (e) *Exuviaella aequatorialis* (redrawn after Hasle 1960). (f) *Prorocentrum sphaeroideum* (redrawn after Schiller 1918). (g) *Prorocentrum nanum* (redrawn after Schiller 1918). (h) *Prorocentrum pusillum* (redrawn after Schiller 1928). (i) *Prorocentrum ovum* (redrawn after Schiller 1918). (j) *Prorocentrum rotundatum* (redrawn after Schiller 1918). (k) *Prorocentrum cornutum* (redrawn after Schiller 1918). (l) *Prorocentrum cordiforme* (redrawn from Bursa 1959). (m) *Prorocentrum antarcticum* (redrawn after Hada 1970). (n) *Prorocentrum antarcticum* (redrawn after Balech 1976). (o) *Prorocentrum nux* (redrawn after Puigserver & Zingone 2002). (p) *Prorocentrum ponticum* (schematic drawing based on SEM images of Krakhmalny & Terenko 2004).

ultrastructural details of the periflagellar area are needed to better work out apomorphic traits of the phylogenetic clades.

Ultimately, the taxonomy of all small species of *Prorocentrum* must be clarified (except *P. pervagatum*), preferably using an epitypification approach based on material from the corresponding type localities (Kretschmann *et al*. 2018b; Tillmann *et al*. 2021). This is sheer overwhelming work, but it is necessary for the unambiguous application of the names and to largely avoid subjective interpretations in the future. Only a reliable taxonomy enables meaningful applied research on the ecology, biogeography, or toxicology of species in the microbial domain.

ACKNOWLEDGMENTS

Anne Müller (AWI Bremerhaven, Germany) is thanked for continued support in laboratory work. This work was supported by funding by the PACES II research program of the Alfred-Wegener-Institute as part of the Helmholtz Foundation initiative in Earth and Environment. Open Access funding enabled and organized by Projekt DEAL.

REFERENCES

Adachi, M., Sako, Y. and Ishida, Y. 1996. Analysis of *Alexandrium* (Dinophyceae) species using sequences of the 5.8S ribosomal DNA and internal transcribed spacer regions. *J. Phycol.* **32**: 424–32.

Adachi, R. 1972. A taxonomical study of the red tide organisms. *J. Fac. Fish. Pref. Univ. Mie* **9**: 9–145.

Balech, E. 1976. *Clave Ilustrada de Dinoflagelados Antárticos*. Instituto Antartico Argentino Direccion Nacional Del Antartico, Buenos Aires.

Bolinesi, F., Saggiomo, M., Aceto, S. *et al*. 2020. On the relationship between a novel *Prorocentrum* sp. and colonial *Phaeocystis antarctica* under iron and vitamin B_{12} limitation: ecological implications for antarctic waters. *Appl. Sci.* **10**: 6965.

Bursa, A. S. 1959. The genus *Prorocentrum* Ehrenberg. Morphodynamics, protoplasmic structure, and taxonomy. *Can. J. Bot.* **37**: 1–31.

Chacón, J. and Gottschling, M. 2020. Dawn of the dinophytes: a first attempt to date origin and diversification of harmful algae. *Harmful Algae* **97**: 101871.

Chomérat, N., Gatti, C. M. I., Nézan, E. and Chinain, M. 2017. Studies on the benthic genus *Sinophysis* (Dinophysales, Dinophyceae) II. *S. canaliculata* from Rapa Island (French Polynesia). *Phycologia* **56**: 193–203.

Chomérat, N., Bilien, G. and Zentz, F. 2019. A taxonomical study of benthic *Prorocentrum* species (Prorocentrales, Dinophyceae) from Anse Dufour (Martinique Island, eastern Caribbean Sea). *Mar. Biodivers.* **49**: 1299–319.

Dodge, J. D. and Bibby, B. T. 1973. The Prorocentrales (Dinophyceae) I. a comparative account of fine structure in the genera *Prorocentrum* and *Exuviaella*. *Bot. J. Linn. Soc.* **67**: 175–87.

Dodge, J. D. 1975. The Prorocentrales (Dinophyceae). II revision of the taxonomy within the genus *Prorocentrum*. *Bot. J. Linn. Soc.* **71**: 103–25.

Faust, M. A., Larsen, J. and Moestrup, O. 1999. Leaflet no 184. Potentially toxic phytoplankton 3. Genus *Prorocentrum* (Dinophyceae). *In* Lindley, J. A. (Ed.). *ICES Identification Leaflets for Plankton*. International Council for the Exploration of the Sea, Copenhagen, pp. 1–24.

Fensome, R. A., Taylor, F. J. R., Norris, G., Sarjeant, W. A. S., Wharton, D. I. and Williams, G. L. 1993. A classification of living and fossil dinoflagellates. *Micropaleontol. Spec. Pub.* **7**: 1–351.

Fritz, L. and Triemer, R. E. 1985. A rapid simple technique utilizing Calcofluor white M2R for the visualization of dinoflagellate thecal plates. *J. Phycol.* **21**: 662–4.

Gómez, F., Claustre, H. and Souissi, S. 2008. Rarely reported dinoflagellates of the genera *Ceratium*, *Gloeodinium*, *Histoneis*, *Oxytoxum* and *Prorocentrum* (Dinophyceae) from the open Southeast Pacific Ocean. *Rev. Biol. Mar. Oceanogr.* **43**: 25–40.

Gómez, F., Zhang, H., Roselli, L. and Lin, S. 2021. Detection of *Prorocentrum shikokuense* in the Mediterranean Sea and evidence that *P. dentatum*, *P. obtusidens* and *P. shikokuense* are three different species (Prorocentrales, Dinophyceae). *Acta Protozool.* **60**: 47–59.

Gottschling, M., Chacón, J., Žerdoner Čalasan, A. *et al*. 2020. Phylogenetic placement of environmental sequences using taxonomically reliable databases helps to rigorously assess dinophyte biodiversity in Bavarian lakes (Germany). *Freshw. Biol.* **65**: 193–208.

Guiry, M. D. and Guiry, G. M. 2022. *AlgaeBase. World-Wide Electronic Publication*. National University of Ireland, Galway. http://www.algaebase.org searched on 10 February 2022.

Hada, Y. 1970. The protozoan plankton of the Antarctic and Subantarctic seas, JARE. *Sci. Rep. Ser. E, Biol.* **31**: 1–51.

Hansen, P. J. and Tillmann, U. 2020. Mixotrophy in dinoflagellates: prey selection, physiology and ecological importance. *In* Subba Rao, D. V. (Ed.). *Dinoflagellates: Classification, Evolution, Physiology, and Ecological Significance*. Nova Science Publishers, New York, pp. 201–60.

Hasle, G. R. 1960. Phytoplankton and ciliate species from the tropical Pacific. *Skrifter Utgitt Av De Norske Videnskaps-Akademi I Oslo I. mat.-Naturv. Klasse* **2**: 1–50.

Heil, C. A., Glibert, P. M. and Fan, C. 2005. *Prorocentrum minimum* (Pavillard) Schiller: a review of a harmful algal bloom species of growing worldwide importance. *Harmful Algae* **4**: 449–70.

Honsell, G. and Talarico, L. 1985. The importance of flagellar arrangement and insertion in the interpretation of the theca of *Prorocentrum* (Dinophyceae). *Bot. Mar.* **28**: 15–21.

Hoppenrath, M., Elbrächter, M. and Drebes, G. 2009. *Marine Phytoplankton. Selected Microphytoplankton Species from the North Sea around Helgoland and Sylt. E*. Schweizerbart'sche Verlagsbuchhandlung (Nägele und Obermiller), Stuttgart.

Hoppenrath, M., Chomérat, N., Horiguchi, T., Schweikert, M., Nagahama, Y. and Murray, S. 2013. Taxonomy and phylogeny of the benthic *Prorocentrum* species (Dinophyceae) – a proposal and review. *Harmful Algae* **27**: 1–28.

Katoh, K. and Standley, D. M. 2013. MAFFT multiple sequence alignment software version 7: improvements in performance and usability. *Mol. Biol. Evol.* **30**: 772–80.

Keller, M. D., Selvin, R. C., Claus, W. and Guillard, R. R. L. 1987. Media for the culture of oceanic ultraphytoplankton. *J. Phycol.* **23**: 633–8.

Krakhmalny, A. and Terenko, G. V. 2004. *Prorocentrum ponticus* Krachmalny & Terenko sp. nov., a new species of Dinophyta from the Black Sea. *Int J Algae* **6**: 35–42.

Krakhmalny, A. F., Tishaeva, M. V., Panina, Z. A. and Krakhmalny, M. A. 2004. A problem on identity *Prorocentrum cordatum* (Ostf.) Dodge and *P. minimum* (Pavill.) Schiller (Dinophyta). *Int J Algae* **6**: 331–40.

Kretschmann, J., Owsianny, P. M., Žerdoner Čalasan, A. and Gottschling, M. 2018a. The hot spot in a cold environment: puzzling *Parvodinium* (Peridiniopsidaceae, Peridiniales) from the polish Tatra Mountains. *Protist* **169**: 206–30.

Kretschmann, J., Žerdoner Čalasan, A., Kusber, W.-H. and Gottschling, M. 2018b. Still curling after all these years: *Glenodinium apiculatum* Ehrenb. (Peridiniales, Dinophyceae) repeatedly found at its type locality in Berlin (Germany). *Syst. Biodivers.* **16**: 200–9.

Larsen, J. and Nguyen-Ngoc, L. 2004. Potentially toxic microalgae of Vietnamese waters. *Opera Botan.* **140**: 5–216.

Loeblich, A. R. III 1976. Dinoflagellate evolution: speculation and evidence. *J. Protozool.* **23**: 13–28.

Lohmann, H. 1908. Untersuchungen zur Feststellung des vollständigen Gehaltes des Meeres an Plankton. *Wiss. Meeresunters.* **10**: 129–370.

Matzenauer, L. 1933. Die Dinoflagellates des Indischen Ozeans. *Bot. Arch.* **35**: 437–510.

Medlin, L., Elwood, H. J., Stickel, S. and Sogin, M. L. 1988. The characterization of enzymatically amplified eukaryotic 16S-like rRNA-coding regions. *Gene* **71**: 491–9.

Miller, M. A., Pfeiffer, W. and Schwartz, T. 2010. Creating the CIPRES Science Gateway for Inference of Large Phylogenetic Trees. *In* Proceedings of the Gateway Computing Environments Workshop (GCE); New Orleans, pp. 1–8.

Monti, M., Stoecker, D. K., Cataletto, B. and Talarico, L. 2010. Morphology of the flagellar pore complex in *Prorocentrum minimum* (Dinophyceae) from the Adriatic and Baltic seas. *Bot. Mar.* **53**: 357–65.

Murray, S., Ip, C. L., Moore, R., Nagahama, Y. and Fukuyo, Y. 2009. Are prorocentroid dinoflagellates monophyletic? A study of 25 species based on nuclear and mitochondial genes. *Protist* **160**: 245–64.

Osorio-Tafall, B. F. 1942. Notas sobre algunos dinoflagelados planctonicos marinos de México, con descripción de nuevas especies. *An. Esc. Nac. Cienc. Biol.* **11**: 435–47.

Ostenfeld, C. H. 1902. Phytoplankton fra det Kaspiske Hav. *Videnskabelige Meddelelser Dra Dansk Naturhistorisk Forening* **1901**: 129–39.

Pavillard, J. 1916. Recherches sur les Péridiniens du Golfe du Lion. *Travail de l' Institut de Botanique de l' Université de Montpellier et de la Station Zoologique de Cette, Série Mixte, Mémoire* **4**: 1–70.

Pertola, S., Faust, M. A., Kuosa, H. and Hällfors, G. 2003. Morphology of *Prorocentrum minimum* (Dinophyceae) in the Baltic Sea and in Chesapeake Bay: comparison of cell shapes and thecal ornamentation. *Bot. Mar.* **46**: 477–86.

Puigserver, M. and Zingone, A. 2002. *Prorocentrum nux* sp. nov. (Dinophyceae), a small planktonic dinoflagellate from the

Mediterranean Sea, and discussion of *P. nanum* and *P. pusillum*. *Phycologia* **41**: 29–38.
Schiller, J. 1918. Über neue *Prorocentrum*- und *Exuviella*-Arten aus der Adria. *Arch. Protistenkd.* **38**: 250–62.
Schiller, J. 1928. Die planktische Vegetationen des adriatischen Meeres. C. Dinoflagellata I Teil. Adiniferidae, Dinophysidaceae. *Arch. Protistenkd.* **61**: 46–91.
Schiller, J. 1933. Dinoflagellatae (Peridineae) in monographischer Behandlung. In Kolkwitz, R. (Ed.) *Dr. L. Rabenhorst's Kryptogamen-Flora von Deutschland, Österreich und der Schweiz*; Akademische Verlagsgesellschaft, Leipzig, pp. 1–615.
Scholin, C. A., Herzog, M., Sogin, M. and Anderson, D. M. 1994. Identification of group- and strain-specific genetic markers for globally distributed *Alexandrium* (Dinophyceae). II. Sequence analysis of a fragment of the LSU rRNA gene. *J. Phycol.* **30**: 999–1011.
Schröder, B. 1900. Das Phytoplankton des Golfes von Neapel nebst vergleichenden Ausblicken auf das des atlantischen Oceans. *Mitteilungen aus der Zoologischen Station zu Neapel* **14**: 1-38, 1 pl.
Shin, H. H., Li, Z., Mertens, K. N. *et al.* 2019. *Prorocentrum shikokuense* Hada and *P. donghaiense* Lu are junior synonyms of *P. obtusidens* Schiller, but not of *P. dentatum* stein (Prorocentrales, Dinophyceae). *Harmful Algae* **89**: 101686.
Starr, R. C. and Zeikus, J. A. 1993. UTEX – the culture collection of algae at the University of Texas at Austin: 1993 list of cultures. *J. Phycol.* **29**: 1–106.
Steidinger, K. A. and Tangen, K. 1996. Dinoflagelates. *In* Tomas, C. R. (Ed.). *Identifying Marine Diatoms and Dinoflagellates*. Academic Press, San Diego, pp. 387–570.
Taylor, F. J. R. 1976. Dinoflagellates from the international Indian Ocean 1976 expedition. *Bibl. Bot.* **132**: 1–234.
Taylor, F. J. R. 1980. On dinoflagellate evolution. *Biosystems* **13**: 65–108.
Tillmann, U., Salas, R., Gottschling, M., Krock, B., O'Driscoll, D. and Elbrächter, M. 2012. *Amphidoma languida* sp. nov. (Dinophyceae) reveals a close relationship between *Amphidoma* and *Azadinium*. *Protist* **163**: 701–19.
Tillmann, U., Trefault, N., Krock, B., Parada-Pozo, G., De la Iglesia, R. and Vásquez, M. 2017. Identification of *Azadinium poporum* (Dinophyceae) in the Southeast Pacific: morphology, molecular phylogeny, and azaspiracid profile characterization. *J. Plankton Res.* **39**: 350–67.
Tillmann, U., Hoppenrath, M. and Gottschling, M. 2019. Reliable determination of *Prorocentrum micans* Ehrenb. (Prorocentrales, Dinophyceae) based on newly collected material from the type locality. *Eur. J. Phycol.* **54**: 417–31.
Tillmann, U., Wietkamp, S., Krock, B., Tillmann, A., Voss, D. and Gu, H. 2020. Amphidomataceae (Dinophyceae) in the western Greenland area, including the description of *Azadinium perforatum* sp. nov. *Phycologia* **59**: 63–88.
Tillmann, U., Bantle, A., Krock, B., Elbrächter, M. and Gottschling, M. 2021. Recommendations for epitypification of dinophytes exemplified by *Lingulodinium polyedra* and molecular phylogenetics of the Gonyaulacales based on curated rRNA sequence data. *Harmful Algae* **104**: 101956.
Tillmann, U., Beran, A., Gottschling, M., Wietkamp, S. and Hoppenrath, M. 2022. Clarifying confusion – *Prorocentrum triestinum* J. Schiller and *Prorocentrum redfieldii* Bursa (Prorocentrales, Dinophyceae) are two different species. *Eur. J. Phycol.* **57**: 207–26.
Velikova, V. and Larsen, J. 1999. The *Prorocentrum cordatum*/-*Prorocentrum minimum* taxonomic problem. *Grana* **38**: 108–12.
Wulff, A. 1916. Über das Kleinplankton der Barentssee. *Wissenschaftliche Meeresuntersuchungen, Neue Folge, Abteilung Helgoland* **13**: 95–125.
Žerdoner Čalasan, A., Kretschmann, J. and Gottschling, M. 2020. Contemporary integrative taxonomy for sexually-deprived protists: a case study of *Trachelomonas* Ehrenb. (Euglenaceae) from Western Ukraine. *Taxon* **69**: 28–42.

SUPPORTING INFORMATION

Additional Supporting Information may be found in the online version of this article at the publisher's web-site:

Fig. S1: *Prorocentrum pervagatum* sp. nov. (strain CA-01), LM micrographs. **Fig. S2**: *Prorocentrum pervagatum* sp. nov. (strain CA-01), SEM micrographs, first set. **Fig. S3**: *Prorocentrum pervagatum* sp. nov. (strain CA-01), SEM micrographs, second set. **Fig. S4**: *Prorocentrum pervagatum* sp. nov. (strain P3-B7), LM and SEM micrographs. **Fig. S5**: *Prorocentrum pervagatum* sp. nov. (strain P3-C7), LM and SEM micrographs. **Fig. S6**: *Prorocentrum pervagatum* sp. nov. (strain LP-D3), LM micrographs. **Fig. S7**: *Prorocentrum pervagatum* sp. nov. (strain LP-D3), SEM micrographs. **Fig. S8**: *Prorocentrum pervagatum* sp. nov. (strain LP-D10), LM micrographs. **Fig. S9**: *Prorocentrum pervagatum* sp. nov. (strain LP-D10), SEM micrographs. **Table S1**: Voucher information on strains used in the phylogenetic analysis.